



Universiteit  
Leiden  
The Netherlands

## Exploring kidney organoid vascularization

Koning, M.

### Citation

Koning, M. (2026, February 4). *Exploring kidney organoid vascularization*. Retrieved from <https://hdl.handle.net/1887/4288745>

Version: Publisher's Version

License: [Licence agreement concerning inclusion of doctoral thesis in the Institutional Repository of the University of Leiden](#)

Downloaded from: <https://hdl.handle.net/1887/4288745>

**Note:** To cite this publication please use the final published version (if applicable).



# CHAPTER 6

---

## Single cell transcriptomics of human kidney organoid endothelium reveals vessel growth processes and arterial maturation upon transplantation

M. Koning\*, S.J. Dumas\*, E. Meta, E. Lievers, A.M.A. de Graaf,  
M. Borri, L.J. Nai Chung Tong, X. Liang, P. Liu, F. Chen, L. Lin, Y. Luo,  
P. Carmeliet, C.W. van den Berg, A.J. Rabelink

\* authors contributed equally to the work

*NPJ Regenerative Medicine, 2025*

## Abstract

Kidney organoids derived from human induced pluripotent stem cells lack a proper vasculature, hampering their applicability. Transplantation prevents the loss of organoid endothelial cells (ECs) observed *in vitro*, and promotes vascularization. In this study, we transplanted kidney organoids in chicken embryos and deployed single-cell RNA sequencing of ~12,000 organoid ECs to delineate their molecular landscape and identify key changes associated with transplantation. Transplantation significantly altered EC phenotypic composition. Consistent with angiogenesis, proliferating EC populations expanded 8 days after transplantation. Importantly, ECs underwent a major vein-to-arterial phenotypic shift. One of the transplantation-specific arterial EC populations, characterized by laminar shear stress response and Notch signalling, showed a similar transcriptome as human fetal kidney arterial/afferent arteriolar ECs. Consistently, transplantation-induced transcriptional changes involved proangiogenic and arteriogenic SOX7 transcription factor upregulation and regulon enrichment. These findings point to blood flow and candidate transcription factors such as SOX7 as possible targets to enhance kidney organoid vascularization.

## Introduction

The absence of a functional vasculature in cultured human induced pluripotent stem cell (hiPSC)-derived kidney organoids is a major limitation. It precludes full maturation and functionality of organoid nephron structures, thus restricting their applicability. In organoids maintained *in vitro*, the sparse endothelial cells (ECs) that are initially formed during differentiation perish over time, suggesting the absence of essential cues for EC maintenance in the culture conditions. We have previously shown that transplantation in the coelomic cavity of chicken embryos induces functional vascularization and enhanced maturation of kidney organoids. Interestingly, the vasculature in these transplanted organoids is chimeric, consisting of both chicken and human ECs which, contrary to the *in vitro* situation, are maintained *in vivo*. To date, it is unclear what leads to the demise of human ECs *in vitro* as well as what sustains them upon transplantation.

Renal ECs are known to display extensive molecular and phenotypic heterogeneity to support the specific functions of each nephron segment<sup>1-4</sup>. Glomerular ECs display fenestrae without diaphragms and play a role in glomerular filtration. ECs in peritubular capillaries have bridged fenestrae and contribute to the tubular reabsorption of solutes. In the larger renal vessels, the EC lining is continuous. A recent study demonstrated that renal EC heterogeneity is even more extensive than was previously thought by identifying at least 24 distinct renal EC phenotypes in the adult mouse kidney based on single cell RNA sequencing (scRNAseq) analysis<sup>1</sup>. However, it is unknown whether and to what extent kidney organoid-derived ECs resemble renal ECs. Although previous studies provided scRNA-seq data of kidney organoid cells, the absence or paucity of ECs recovered from the organoids precluded the extensive analysis of this critical cell population. In this study, we isolated a total of 11,966 high-quality human ECs from untransplanted and transplanted kidney organoids and analyzed them using scRNAseq. We demonstrate that organoid ECs *in vitro* display phenotypic heterogeneity, but lack similarity to fetal kidney ECs. Transplantation in chicken embryos stimulates EC proliferation and induces a new, more mature, arterial EC phenotype, resembling fetal kidney arterial-afferent arteriolar ECs.

## Results

### ***Transplantation greatly affects the kidney organoid endothelial cell transcriptome***

To evaluate the molecular effects of transplantation on kidney organoid ECs, we compared human ECs from organoids cultured *in vitro* with those from organoids transplanted in chicken embryos. HiPSCs were differentiated to kidney organoids using a

previously published protocol (Fig 1a, step 1)<sup>5</sup>. On day 7+12 of differentiation they were either transplanted in the coelomic cavity of Hamburger Hamilton stage 22-23 (HH22-23) chicken embryos or maintained in vitro (Fig 1a, step 2). This timepoint was selected to ensure the presence of endogenous ECs in the organoids at the time of transplantation<sup>6</sup>. On day 7+13 and d7+20 of differentiation, transplanted organoids and untransplanted controls were collected for analysis. The 24 h post-transplantation timepoint was included to isolate the effects of the microenvironmental changes resulting from transplantation, from the effects of blood perfusion, which we observe throughout the organoids from day 3 after transplantation<sup>6</sup>. Since kidney organoids contain a limited number of ECs, in-depth scRNAseq analysis of these cells requires their enrichment. We therefore isolated ECs from dissociated organoids through fluorescence activated cell sorting (FACS) using human CD31 as EC marker for purification (Fig 1a, step 3). Sorted ECs were processed for sequencing. After quality control and EC filtering, a total of 11,966 high quality human ECs were subjected to downstream analyses: 2777 and 1505 ECs from untransplanted d7+13 and d7+20 organoids, and 307 and 7377 ECs from transplanted D7+13 and d7+20 organoids, respectively (Fig 1b, supplementary Fig. 1, supplementary data 1). Correlation analysis demonstrated that both time and transplantation altered organoid EC transcriptomes, with the latter having a greater impact (Fig 1c). We identified significantly differentially expressed genes in each condition (supplementary data 2, Fig 1d). Subsequent geneset enrichment analysis (GSEA) revealed that in organoids cultured in vitro, ECs at d7+13 upregulated genes associated with aerobic respiration (e.g. *NDUFC2*, *ATP5PO*, *NDUFB8*), and active replication, whereas at d7+20, upregulation of genes associated with DNA damage/growth arrest (e.g. *CDKN1A*, *CCND1*, *MDM2*, *SNAI2*) was observed. Upon transplantation, ECs at d7+13 upregulated genes associated with glycolysis (e.g. *SLC2A1*, *LDHA*, *ENO1*, *ENO2*, *ALDOA*, *PGK1*) rather than oxidative phosphorylation, along with hypoxia-induced genes (e.g. *BNIP3*, *FAM162A*) (Fig. 1e, supplementary data 3). This metabolic transcriptome shift from aerobic respiration to glycolysis is consistent with the change in environment from in vitro culture at 21% oxygen to the hypoxic coelomic cavity. Eight days after transplantation, genes associated with angiogenesis (e.g. *EPAS1*, *AQP1*, *GJA5*, *ESM1*), blood coagulation (e.g. *MYL9*), circulation (e.g. *EPAS1*, *GJA5*), matrix deposition (e.g. *COL12A1*), and antigen presentation (e.g. *HLA-B*, *B2M*, *HLA-C*), were upregulated, indicating vessel growth, response to blood perfusion and interaction with the host immune system (Fig. 1d, e, supplementary data 3).

To identify the potential drivers of the transcriptional phenotypes adopted by kidney organoid ECs in these 4 conditions, transcription factor inference analysis was conducted using the SCENIC workflow<sup>7</sup>. Our analysis revealed dynamic changes in the expression of specific transcription factors and their regulons (Fig. 1f).

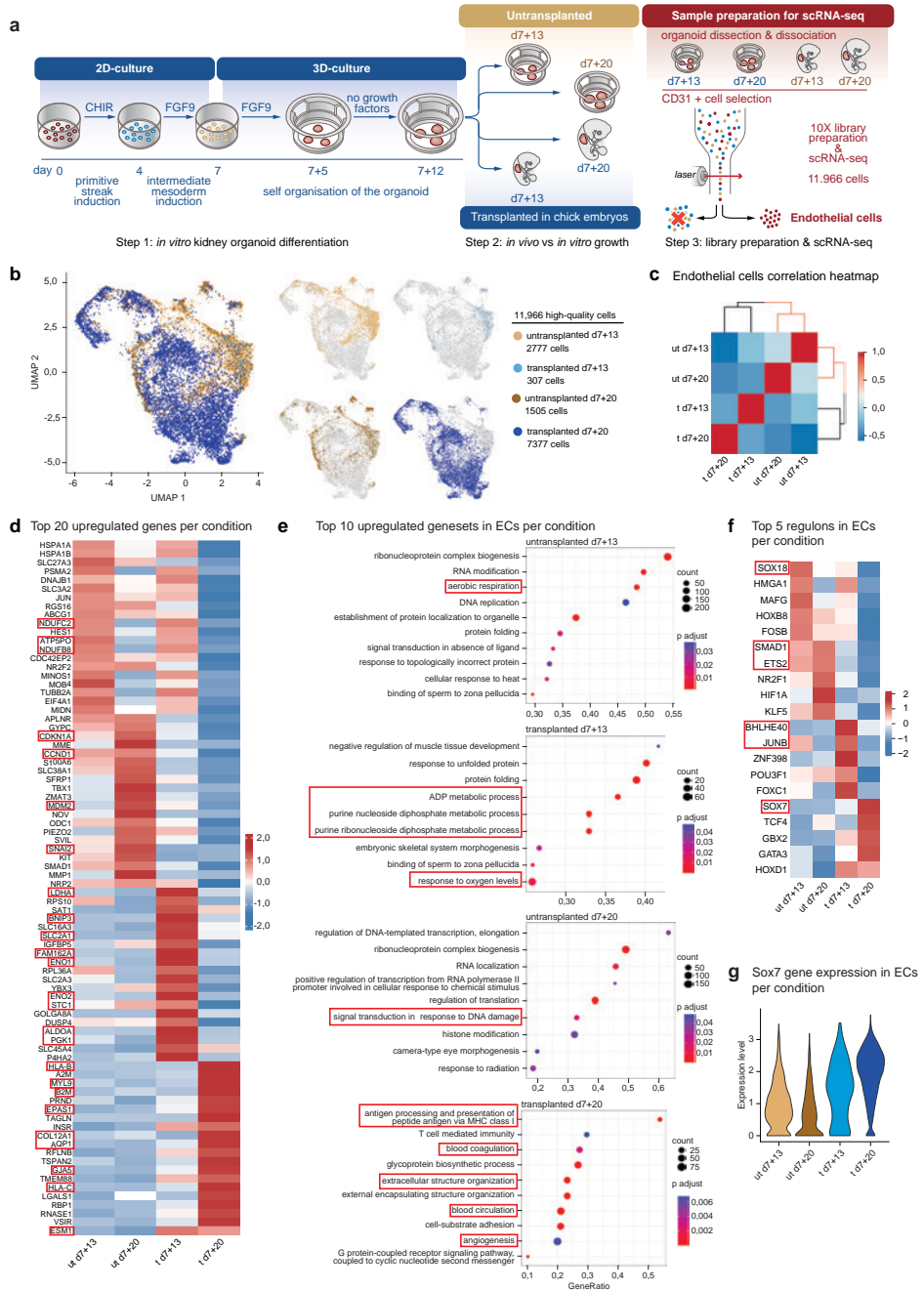


**Figure 1: scRNAseq of enriched ECs from untransplanted and transplanted kidney organoids.** **a** Workflow of step 1: kidney organoid differentiation from hiPSCs, step 2: in vitro culture versus intracoelemic transplantation in chicken embryos, and step 3: organoid collection, dissociation to single cells, endothelial cell enrichment and scRNAseq. **b** UMAP visualization of a total of 11,966 high-quality human endothelial cells obtained from untransplanted (2777 cells from d7+13,

1505 from d7+20) and transplanted (307 cells from d7+13, 7377 from d7+20) kidney organoids, color-coded by condition. **c** Heatmap visualization of similarity analysis of ECs from the different conditions. ECs from each condition had unique transcriptome profiles but showed a higher similarity based on transplantation conditions than timepoints. Scale: z-score of the gene expression level. Abbreviations: ut = untransplanted, t = transplanted. **d** Expression-level scaled heatmap of the top 20 upregulated genes per condition. Highlighted genes are discussed in the text. Scale: z-score of the gene expression level. **e** Top 10 upregulated gene sets in ECs for each condition. Dot size indicates proportion of cells expressing a gene. Color intensity indicates the level of expression. Highlighted gene sets are discussed in the text. **f** Top 5 upregulated regulons in ECs for each condition, generated by transcription factor inference analysis conducted using the SCENIC method. Highlighted regulons are discussed in the text. Scale: z-score of the regulon enrichment score. **g** Violin plot visualization of the expression level of the SOX7 gene in ECs from the different conditions.

At day 7+13, ECs from untransplanted organoids exhibited a significant enrichment of the SOX18 regulon, a transcription factor known for its transient expression during embryonic development, particularly in nascent ECs<sup>9</sup>. This finding suggests activation of SOX18 in the early stages of EC differentiation in kidney organoids *in vitro*. By day 7+20, we observed an upregulation of the SMAD1 and ETS2 regulons in the remaining ECs, transcription factors promoting EC survival and angiogenesis<sup>9,10</sup>. Upon transplantation, we detected an upregulation of the hypoxia-inducible BHLHE40 transcription factor, along with the stress-induced JUNB regulon, consistent with an adaptive response of ECs to the altered microenvironment post-transplantation. At day 7+20 in transplanted organoids, ECs displayed a significant enrichment of the SOX7 regulon as well as SOX7 upregulation (Fig. 1f, g). SOX7 is recognized for its roles in vasculogenesis, angiogenesis during embryonic development, and arterial EC specification<sup>11,12</sup>. This enrichment suggests that SOX7 plays a pivotal role in the maturation and specification of ECs under transplantation conditions, consistent with the observed response to blood perfusion.

### ***Kidney organoid transplantation sustains endothelial cell proliferation***

It is known that ECs in kidney organoids regress over time *in vitro*<sup>13</sup>, whereas they persist upon transplantation<sup>6</sup>. To further investigate possible changes in proliferation, we performed unsupervised clustering of the 11,966 high quality human ECs, which resulted in 13 subclusters (Fig. 2a), each with a distinct transcriptome profile (top marker genes in Fig. 2b and supplementary data 4, marker genes in supplementary data 5). Clusters 1 and 2 both displayed a clear proliferative transcriptome. The distinction between the two clusters was based on cell cycle phases: ECs in cluster 1 showed the highest S phase module score, mainly upregulating genes associated with the G1S-S phase. ECs in cluster 2 showed the highest G2M phase module score, upregulating genes associated with the G2M-M phase (Fig. 2c, d). Clusters 3 to 13 did not exhibit an upregulation of any proliferation genes, indicating rather a quiescent or a migrating cell state.

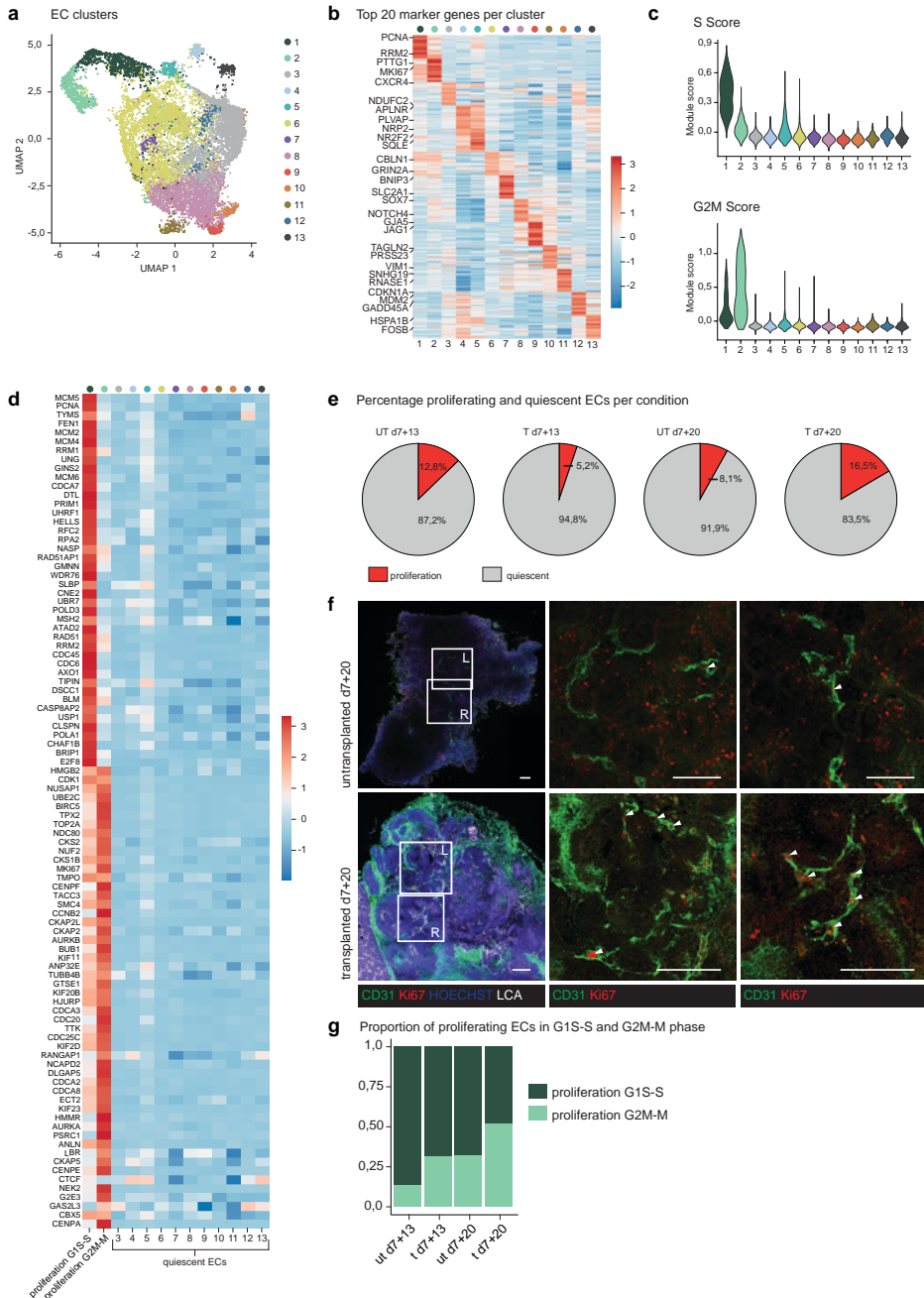


**Figure 2: Endothelial cell proliferation is sustained after transplantation.** **a** UMAP visualization of a total of 11,966 high-quality human endothelial cells obtained from untransplanted (2777 cells from d7+13, 1,505 from d7+20) and transplanted (307 cells from d7+13, 7377 from d7+20) kidney organoids, color-coded by cluster (n=13). **b** Expression-level scaled heatmap of the top 20 marker genes per EC cluster. Scale = z-score of the gene expression level. **c** Violin plots depicting Module scores for S phase (top) and G2M phase (bottom) of the cell cycle for each EC cluster. Cluster 1 displayed the highest S module score, whereas cluster 2 had the highest G2M module score. Cluster 3 – 13 had

low S and G2M scores. **d** Expression-level scaled heatmap of genes associated with proliferation per EC cluster. Cluster 1 and 2 express proliferation genes, with cluster 1 expressing genes associated with G1S-S phase and cluster 2 expressing genes associated with G2M-M phase. Cluster 3-13 did not express proliferation genes and were classified as quiescent EC clusters. Scale = z-score of the gene expression level. **e** Pie charts of the percentage of proliferating (red) and quiescent (grey) ECs per condition. The percentage of proliferating ECs is highest in transplanted day 7+20 organoids. **f** Immunofluorescent images of untransplanted day 7+20 (top) and transplanted d7+20 (bottom) kidney organoids, stained for human CD31 (green) ki67 (red) and HOECHST. Injected LCA (white) is visible in the transplanted organoid. In untransplanted organoids, few proliferating endothelial cells (CD31+, ki67+, arrowheads) can be identified, whereas in transplanted organoids, they appear more abundant. Scale bar: 100 $\mu$ m. Images are based on 3 separate experiments. **g** Bar graph depicting the proportion of proliferating ECs in G1S-S (dark green) and G2M-M (light green) phase per condition.

Comparison of the proportion of proliferating and quiescent or migrating ECs between the different conditions revealed a decrease in proliferating ECs in untransplanted organoids over time, from 12.8% at d7+13 to 8.1% at d7+20, consistent with a decreased proliferative potential of these ECs.

The percentage of proliferating ECs was lowest in transplanted d7+13 organoids (5.2%). This is possibly due to the extensive changes in microenvironment upon transplantation, requiring metabolic rewiring of transplanted ECs and likely affecting their proliferative capacity temporarily. However, in transplanted d7+20 organoids, it had increased to 16.5%, the highest percentage of all conditions, and twice more than its timepoint-matched untransplanted control (Fig. 2e, supplementary data 6). Whole-mount staining of untransplanted and transplanted day 7+20 organoids with proliferative marker Ki67 (whose gene showed upregulation in the G2M-M proliferating cluster, as shown in supplementary Fig. 2a) and CD31, validated the presence of proliferating human CD31+Ki67+ ECs in both experimental settings (Fig. 2f, supplementary data 7), which appeared more abundant in transplanted organoids. Interestingly, the proportion of proliferating ECs in G2M-M phase was higher in transplanted organoids compared with untransplanted organoids (Fig. 2g). The lower percentage of proliferating ECs, in particular in G2M-M phase in untransplanted organoids, might be due to cell cycle arrest as a result of DNA damage (Fig. 1e), and could underlie the declining number of ECs in culture in vitro.

### ***Heterogeneity and phenotypic changes in organoid ECs upon transplantation***

Next, we investigated the characteristics of the quiescent or migrating EC clusters. In order to determine EC phenotype identity, we first calculated artery, vein and lymphatic module scores for the ECs in each subcluster based on known canonical marker genes. With this approach, 4 artery clusters (artery 1-4), 1 vein cluster, 1 lymphatic cluster and 5 capillary clusters (capillary 1-5 – not showing artery, vein or lymphatic phenotypes) were identified

(Fig. 3a). The identity of these subclusters was confirmed by their upregulated expression of artery, vein and lymphatic canonical marker genes (Fig. 3b). Unsupervised hierarchical clustering provided further support by grouping the vein with the lymphatic cluster, and the artery clusters together. Capillary 1,4 and 5 were more similar to the vein and lymphatic clusters while capillary 2 and 3 showed a stronger resemblance to the proliferating EC clusters (Fig. 3c). Untransplanted organoids contained mainly capillary ECs (d7+13 86.5%, d7+20 87.4%), some venous (d7+13 6.4%, d7+20 6.6%) and lymphatic (d7+13 5.7%, d7+20 4.6%) ECs and a very small amount of arterial ECs (d7+13 1.3%, d7+20 1.4%). In transplanted d7+13 organoids, the proportions were similar, with a slight decrease in venous and lymphatic ECs in favor of capillary and arterial ECs.

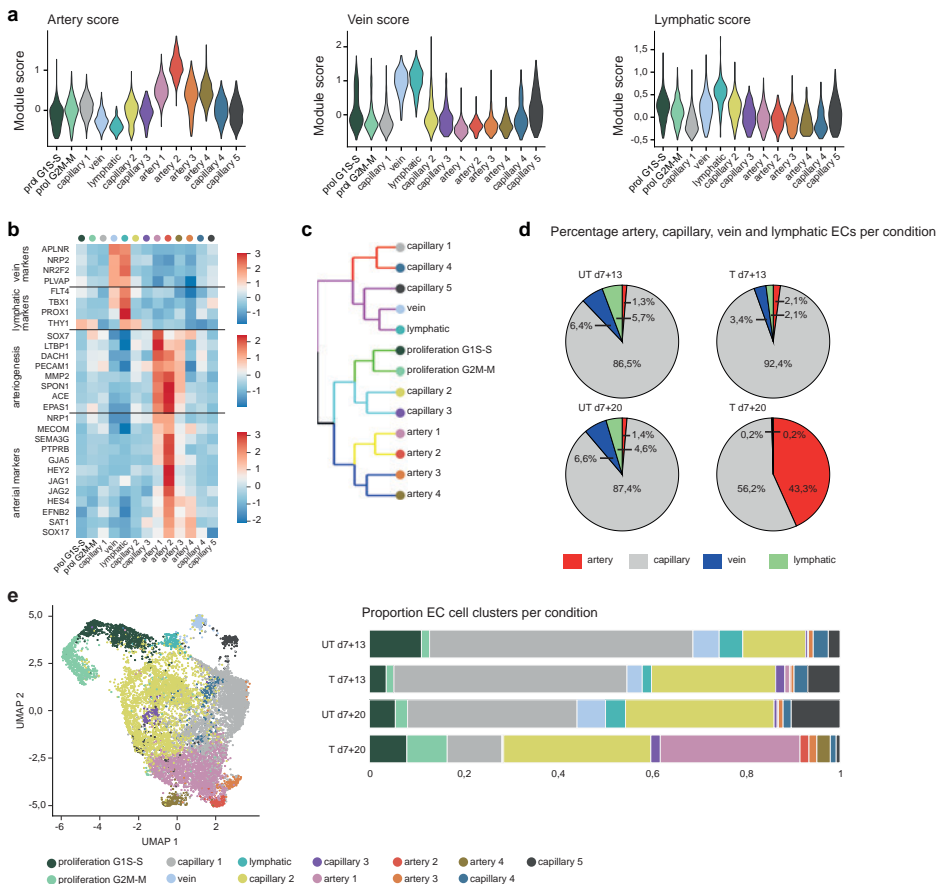


**Figure 3: Kidney organoids contain venous, lymphatic, arterial and capillary ECs and transplantation induces a switch from venous to arterial phenotype.** **a** Violin plots depicting artery (left), vein (middle) and lymphatic (right) module scores for each EC cluster. 4 artery clusters (artery 1-4), 1 vein cluster, 1 lymphatic cluster and 5 capillary clusters can be distinguished. **b** Expression-level scaled heatmap of vein, lymphatic, arteriogenesis and arterial markers per EC cluster. Scale: z-score of the gene expression level. **c** Hierarchical clustering of EC clusters, color-

coded according to p-value from multiscale bootstrap resampling analysis on all highly variable genes. **d** Pie charts of the percentage of artery (red), capillary (grey), vein (blue) and lymphatic (green) ECs per condition. There is a large increase in the percentage of arterial ECs in transplanted day 7+20 organoids, while vein, lymphatic and capillary ECs are reduced in this condition. **e** Relative cluster quantification for each condition, showing a significant decrease in capillary 1 and 5 clusters and a significant increase in artery cluster 1,2 and 4 in transplanted day 7+20 organoids compared to the other conditions (untransplanted and transplanted d7+13 and untransplanted d7+20)

Eight days after transplantation, however, a striking shift from venous and capillary to arterial ECs had occurred, resulting in 43.3% arterial ECs, 56.2% capillary ECs and only 0.2% vein and lymphatic ECs (Fig. 3d, supplementary data 8). Further analysis of the artery subtypes revealed that the artery 1,2 and 4 clusters were nearly absent in untransplanted organoids and mostly appeared upon transplantation (Fig. 3e, supplementary data 9). The top marker genes for each of the artery clusters revealed artery 1 to represent an immature artery EC phenotype, artery 2 to express more mature artery EC markers, and artery 3 and 4 to upregulate endoMT markers including smad2/3-dependent TGFB target genes, with artery 4 showing a decreased expression of EC markers (Fig. 3b, supplementary Fig. 3a). Regarding capillary phenotypes, the proportion of capillary 1 and 5 ECs, characterized by the high expression level of OXPHOS genes and of response-to-stress and DNA damage genes, respectively, was decreased after transplantation at d7+20 (Fig. 3e, supplementary Fig. 3b, c). Capillary 3 EC cluster showing a robust glycolytic and a response-to-hypoxia phenotype was only observed in transplanted organoids, as also previously reported in podocytes upon kidney organoid transplantation (Fig. 3e, supplementary Fig. 3d)<sup>6</sup>. The proportion of the capillary 2 cluster, for which the phenotype was unclear, and capillary 4 cluster, with a response-to-DNA damage without activation of a response-to-stress gene signature, didn't seem much affected by the transplantation or timepoint (Fig. 3e, supplementary Fig. 3c). To summarize, ECs in kidney organoids did not represent a homogeneous population, but displayed heterogeneity consistent with arteriovenous specification, with transplantation inducing a dramatic shift to an arterial phenotype.

### ***Tissue-specification of organoid ECs and similarities with fetal kidney ECs***

In vivo, ECs display tissue-specific molecular features to support development and homeostasis. To assess the renal specification of kidney organoid ECs, we analyzed enrichment of human liver, spleen, skin, heart, pancreas, muscle, lung, vasculature, and kidney EC marker genes, identified from the Tabula Sapiens dataset<sup>14</sup> (supplementary Fig. 4, supplementary data 10), in organoid ECs. Kidney organoid ECs showed the highest enrichment of kidney-specific markers compared to EC markers from other

tissues, especially after transplantation (Fig. 4a). However, they also expressed marker genes associated with ECs from other tissues, including the liver, pancreas, and muscle, indicating that the tissue-specific differentiation of kidney organoid ECs is incomplete under all tested conditions (Fig. 4a).

In order to perform an in-depth comparison of organoid ECs with fetal kidney ECs, a human fetal kidney EC reference was created from publicly available scRNA-seq data resulting in a dataset of 3155 fetal kidney ECs from 8 to 17 weeks of gestation (Fig. 4b). Unsupervised subclustering resulted in 7 distinct subclusters: artery-afferent arteriole, glomeruli, efferent arteriole, capillary, vein, lymphatic and proliferation ECs (Fig. 4c,d, marker genes in supplementary data 11). Integration and co-embedding of fetal kidney and organoid ECs revealed limited overlap between the EC clusters (Fig. 4e). However, 2 organoid EC types did display similarity to fetal kidney ECs: the proliferating ECs, which were enhanced upon transplantation, and the artery ECs that newly appeared in transplanted organoids (Fig. 4e,f). Specifically, organoid proliferation G1S-S and G2M-M clusters resembled the fetal kidney proliferation cluster and organoid artery cluster 2 showed the highest similarity with the fetal kidney artery-afferent arteriole cluster, with 121 common marker genes (Fig. 4g, supplementary data 12). The enhanced renal specification of ECs from transplanted organoids appears therefore associated to the vein-to-artery phenotype shift. Since transplantation enables perfusion of organoid ECs, and shear stress is known to play a role in arterial differentiation *in vivo*<sup>15</sup>, we hypothesized that this was an important factor driving arterial and renal specification of ECs upon transplantation. Indeed, analysis of the expression of laminar shear stress-associated genes by ECs from the different conditions demonstrated that these were highly expressed in transplanted day 7+20 organoids specifically (Fig. 5a). Furthermore, of all EC clusters, artery cluster 2, the cluster with the closest resemblance to fetal kidney arterial ECs, displayed the highest expression of laminar shear stress-associated genes (Fig. 5b). This gene signature suggests that artery cluster 2 consists of perfused ECs. To further investigate this, we identified JAG1, a possible mechanotransducer in ECs<sup>16</sup>, among the top marker genes for the artery 2 cluster that is also restricted to artery/afferent arteriolar ECs amongst fetal kidney ECs (supplementary Fig. 2b, c), and evaluated the effect of laminar flow on its expression by iPSC-derived EC using a bulk RNA-seq dataset that our group has published previously<sup>17</sup>. iPSC-derived ECs cultured under flow for 4 days showed significant upregulation of JAG1 expression compared to those cultured in static culture, supporting the notion that artery cluster 2 represents perfused ECs (Fig. 5c, supplementary data 13).



color-coded by dataset (left) and gestational age (right). **c** UMAP visualization of the fetal kidney EC dataset, color-coded by EC subcluster. 7 clusters could be distinguished: artery-afferent arteriole, glomeruli, efferent arteriole, capillary, vein, lymphatic and proliferation. **d** Dot plot representing marker gene expression in fetal kidney EC clusters. Dot size indicates proportion of cells in cluster expressing a gene, color intensity indicates the level of expression. **e** UMAP visualization of fetal kidney ECs and ECs from transplanted kidney organoids at day 7+20, color-coded by origin (top), and cluster (bottom). **f** Heatmap visualization of the correlation between the different kidney organoid EC clusters and the fetal kidney EC clusters. The organoid proliferation clusters show high similarity to fetal kidney proliferating ECs, and the organoid artery 2 cluster correlates with the fetal kidney artery-afferent arteriole cluster. Scale: correlation coefficient. **g** Venn diagram displaying the overlap between marker genes for transplanted organoid artery 2 ECs and fetal kidney artery-afferent arteriole ECs: These clusters have 121 overlapping marker genes.

Here, we demonstrated that the transplantation of kidney organoids facilitated the differentiation of a subset of endogenous organoid ECs into a phenotype resembling kidney fetal (afferent) arteriolar cells, likely driven by blood perfusion. In contrast, the remaining quiescent organoid ECs exhibited distinct transcriptomic profiles compared to human fetal kidney ECs. Of note, despite the previously demonstrated perfusion of organoid glomeruli upon transplantation, we did not identify an organoid EC cluster with a glomerular gene signature, even in transplanted organoids. However, chicken ECs collected with the transplanted organoids did include a glomerular-like EC cluster (*GATA5* and *EHD3* positive) (supplementary Fig. 6a, b). A limitation of this analysis is that some of the chicken cells in the day 7+20 samples are derived from chicken tissue (liver) that could not be completely removed from the organoid during collection. The chicken glomerular ECs, however, display such a specific gene signature that they are almost certainly derived from the organoid glomeruli and not from the chicken liver.

6

## Discussion

In this study, we provided an in-depth molecular analysis of kidney organoid EC subtypes and their specification in in vitro culture and upon transplantation. Given the scarcity of ECs in organoids, enrichment of ECs from hundreds of untransplanted as well as transplanted organoids was required for this analysis. To facilitate this, we performed intracoelomic transplantation in chicken embryos. Unlike mammalian models, fertilized eggs are affordable and with minimal ethical constraints at early timepoints of development. Furthermore, chicken embryos are easily accessible by opening the egg shell, lack a fully functional immune system<sup>18,19</sup>, and the coelomic cavity is a favorable environment for the vascularization and maturation of embryonic tissues<sup>20-22</sup>. Unlike the commonly practiced transplantation of kidney organoids under the kidney capsule or subcutaneously in mice<sup>5,23-25</sup>, intracoelomic transplantation enables the collection of a high number of transplanted organoids, as demonstrated here and previously published using nearly 200 chicken embryos<sup>6</sup>. The transplantation duration of 8 days was relatively

short compared to murine transplantation models due to our decision to sacrifice the embryos on day 12 of development, before it is believed they start experiencing pain<sup>26</sup>. Although extending the time *in vivo* would likely further improve organoid vascularization and maturation, we have previously shown that 8 days is sufficient for the establishment of a perfused vascular network within the organoids and epithelial cell maturation. To our knowledge, this is currently the only available *in vivo* model allowing such a high yield of ECs required for this study.

Transplantation had a major impact on organoid EC transcriptome. In line with the previously reported progressive loss of ECs in organoids cultured *in vitro*<sup>6,13</sup>, we found a lower proportion of proliferating ECs in untransplanted than transplanted d7+20 organoids. This was especially clear for ECs in the G2M-M cell cycle phases. ECs in untransplanted organoids upregulated genes associated with response to DNA damage and stress as well as those involved in oxidative phosphorylation (OXPHOS). It has been well documented that ECs rely mainly on glycolysis for ATP production<sup>27,28</sup>. One of the advantages of utilizing glycolysis over OXPHOS is the reduced production of reactive oxygen species (ROS), decreasing oxidative stress<sup>29,30</sup>. Production of ROS derived from OXPHOS is promoted by the high oxygen tension from the ambient air (21%), in which kidney organoids are usually cultured. Given the oxidative effect of ROS on DNA, leading to cell cycle arrest and potentially cell death, OXPHOS in ECs from untransplanted organoids may contribute to the loss of ECs in this condition. Further studies targeting these pathways are warranted to investigate this hypothesis. The reason for the higher OXPHOS gene expression in ECs from untransplanted organoids compared to transplanted ones remains unclear, but it may indicate EC immaturity. Indeed, our group previously demonstrated that immature iPSC-derived ECs exhibit an increased number of mitochondria, albeit dysfunctional, compared to mature endothelium. This dysfunction leads to elevated ROS production and ultimately hinders proper maturation<sup>17</sup>. A similar phenomenon could potentially occur in ECs derived from kidney organoids. However, adapting the *in vitro* culture conditions to 5% O<sub>2</sub> to promote glycolysis over OXPHOS, thereby mimicking what likely happens upon kidney organoid transplantation, did not enhance the vasculature. When placed in a hypoxia incubator in 5% O<sub>2</sub> starting from d7+5 or d7+12 of differentiation, kidney organoids showed the same morphology and vasculature compared to organoids cultured in a regular incubator in 21% O<sub>2</sub>. There was no difference in EC volume between the different conditions and glomeruli remained avascular (supplementary Fig. 5). More extensive analysis, such as scRNAseq or metabolic profiling could possibly reveal more subtle differences that remained undetected by the readouts used. Others have reported an increase in ECs in kidney organoids cultured in 'physiological hypoxia' of 7% O<sub>2</sub><sup>31</sup>. Perhaps the difference in oxygen tensions used partly explains the difference in findings.

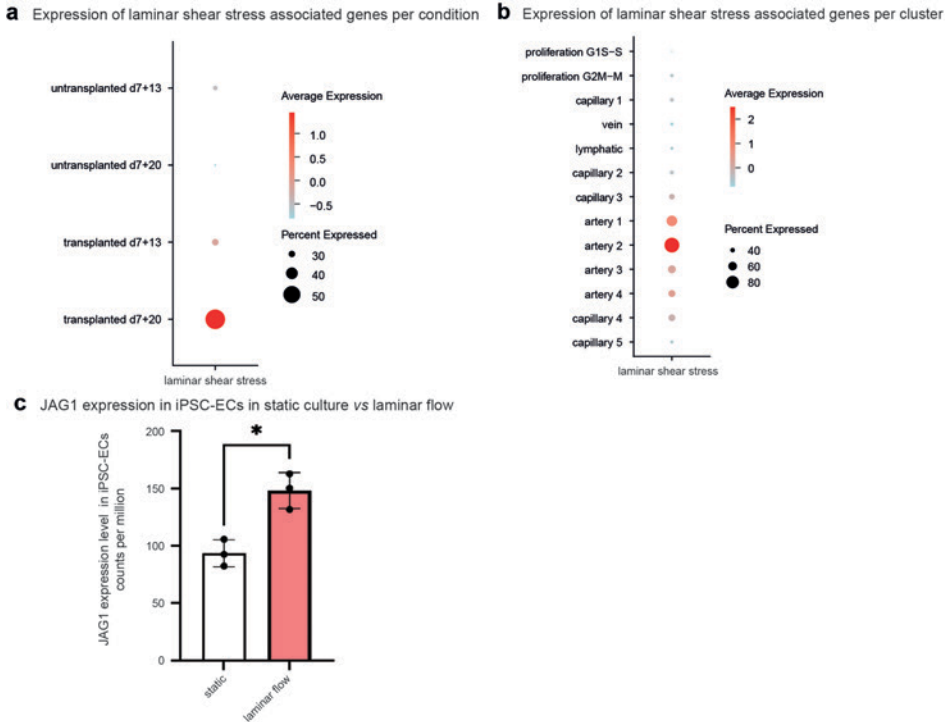


**Figure 5: Upregulation of laminar shear stress associated genes in artery clusters.** **a** Dot plot representing expression of laminar shear stress associated genes in organoid ECs per condition. ECs from transplanted organoids at day 7+20 show the highest expression. Dot size indicates proportion of cells in cluster expressing laminar shear stress associated genes, color intensity indicates the level of expression. **b** Dot plot representing expression of laminar shear stress associated genes in organoid ECs per subcluster. ECs from artery cluster 2 show the highest expression. Dot size indicates proportion of cells in cluster expressing laminar shear stress associated genes, color intensity indicates the level of expression. **c** Bar graph showing the expression of JAG1 in iPSC-derived ECs cultured under static conditions (white) or under laminar flow for 4 days. JAG1 expression is upregulated in ECs under laminar flow.

Arterio-venous specification is an essential aspect of embryonic vascular development and maturation. In kidney organoids *in vitro*, we identified capillary, venous, and lymphatic ECs, while artery ECs were nearly absent. After transplantation, a major shift towards artery ECs occurred. Of note, the proliferating and artery ECs formed clearly distinct clusters, with the proliferating ECs displaying a low artery score. This is consistent with the cell cycle arrest in ECs prior to arterial specification that was reported by others<sup>15</sup>. Although it was previously thought that in early embryology arteries mainly arise by sprouting from existing major arteries<sup>32</sup>, recent lineage tracing studies have shown that arterIALIZATION of venous-featured ECs also plays an important role<sup>33</sup>. This mechanism could partly explain the observed venous to arterial shift upon transplantation. In addition, the shear stress that is induced by perfusion of ECs in transplanted organoids is likely

an important driver of arterIALIZATION. In mouse studies, shear stress has been shown to induce Notch signalling, leading to arterial specification<sup>15</sup>. The upregulated expression of laminar shear stress associated genes in the artery clusters in general, and the artery 2 cluster in particular, supports this theory. Consistent with this observation, another scRNA-seq study on kidney organoid cultured in suspension in spinner flasks, resulting in some levels of flow around and throughout the organoids, identified mostly arterial-like ECs<sup>34</sup>. Comparison of organoid ECs to fetal kidney ECs revealed that the artery 2 EC cluster was the only non-proliferating cluster resembling fetal kidney ECs. This emphasizes the importance of shear stress, implying a role not only in arterial but possibly also for renal specification in kidney organoids. Tissue specification of ECs is partly determined by their angiocrine factor profiles. Interestingly, the importance of blood flow-induced angiocrine signaling has been highlighted in different tissues, such as liver, heart or kidney, during organ development or regeneration<sup>35-37</sup>. Further studies linking blood flow and kidney-specific angiocrine signaling and broader, EC tissue-specification, are warranted to elucidate the underlying mechanisms.

Previously, shear stress was applied to kidney organoids *in vitro* in an attempt to enhance their vascularization<sup>38,39</sup>. Organoids were placed in a microfluidic chip and subjected to flow, resulting in an increase in ECs compared to static conditions and incidentally the appearance of perfusable vessels, reflecting to some extent what is observed upon transplantation<sup>38</sup>. Alternatively, co-culture with human umbilical vein endothelial cell (HUVEC)-coated microfluidic channels led to migration of HUVECs into the organoids and connection to organoid-derived ECs<sup>39</sup>. However, both methods failed to induce functional and glomerular vascularization. This might be partly explained by the location of shear stress, which in the microfluidic chips was applied over the top of the organoids instead of through vessels that connect to pre-existing ECs as it occurs upon transplantation. In co-culture experiments, while the flow was applied to HUVEC coated channels beneath the organoid, the characteristics of the flow and level of shear stress in the sprouting vessels vascularizing the organoid is unknown. Other factors influencing vascularization may have been suboptimal or absent, including the type of ECs used, the timing of vascularization relative to the organoid's developmental stage, or other essential cues.

Although we previously demonstrated that human organoid ECs invade glomerular structures following intracoelomic transplantation, we did not identify a human EC cluster with a glomerular signature in the transplanted organoids in the present study. The discrepancy could be due to the limited duration of transplantation and exposure to blood perfusion, with further EC specialization requiring prolonged transplantation. The previously described slightly cuboidal appearance and lack of fenestrations of organoid

glomerular ECs on transmission electron microscopy (TEM) support this theory<sup>6</sup>. Other possibilities are that the number of intraglomerular human ECs is too small to detect them as a separate cluster and / or that chicken derived ECs are the major contributors to the glomerular vasculature after transplantation. Indeed, chicken ECs collected together with the transplanted organoids<sup>6</sup> included a cluster a glomerular-like ECs (*GATA5* and *EHD3* positive ECs) (supplementary Fig. 6a, b). As no other chicken glomerular cells were detected in the chicken scRNA-seq data<sup>6</sup>, it is unlikely that these glomerular-like ECs resulted from contamination by native chicken kidney tissue during organoid collection. The fact that a subset of chicken ECs attains a glomerular gene signature within 8 days while organoid ECs do not, suggests that endogenous organoid ECs might not be ideally suited for glomerular vascularization. This implies that an external source of ECs might be necessary for optimal vascularization in vitro. Notably, kidney vascularization, including occasional glomerular vascularization with EC-podocyte interactions, was recently achieved in vitro by mixing hiPSCs with transgenic hiPSCs that express an inducible ETS translocation variant 2 (*ETV2*) transcription factor during kidney organoid differentiation<sup>34</sup>. *ETV2* expression is essential for EC specification during embryonic development and its induction in iPSCs directly differentiates them to ECs<sup>40,41</sup>. In this model, differentiation of a subpopulation of iPSCs to ECs without otherwise adapting the kidney organoid protocol was sufficient to enhance organoid (and glomerular) vascularization. This supports the notion that a main cause of the lack of vasculature in kidney organoids in vitro is the ECs themselves and not the (lack of) cues from the surrounding epithelium. Yet, applying flow and hypoxia in this model may further promote (glomerular) vascularization and specify (glomerular) ECs.

In the present study, kidney organoid ECs did not show expression of *ETV2* (*data not shown*) but upregulated *SOX7* transcription factor and regulon in transplanted day 7+20 organoids, compared to all other conditions. *SOX7* is well known for its role in vascular development, hypoxia-induced angiogenesis, and is essential for the establishment of a correct arteriovenous identity during vascular development<sup>27-30</sup>. In this context, *ETV2* and *SOX7* are concomitantly expressed in endothelial progenitor cells with *ETV2* binding directly to *SOX7* promoter to induce its expression<sup>42</sup>. *SOX7* could therefore be a possible target for enhancing kidney organoid vascularization and EC specification. Further studies are required to clarify the role of endothelial *SOX7* in kidney organoid vascularization. Combining hypoxia, shear stress and EC-specific overexpression of *Sox7*, while preventing DNA damage, could be an interesting avenue to explore in order to improve kidney organoid vascularization in vitro.

Our study has some limitations. Using only a single cell line (MAFB iPSC) for the scRNA-seq experiment prevented us from accounting for cell line-specific variations. This might confound the identified EC subclusters and is important to take into account when interpreting the results. Moreover, validation of the different EC subclusters at the protein level was not performed, due to the limited number of cells in each EC cluster per organoid, making this task particularly challenging. Human CD31 was used as a marker for EC enrichment though FACS since kidney organoid ECs display high expression levels of this marker. However, we cannot exclude the presence of CD31-negative early endothelial progenitor cells (EPCs) in the organoids, which were not captured by this approach. Follow-up studies focusing on the process of iPSC-to-EC differentiation should include a marker for EPCs.

In conclusion, transplantation of kidney organoids profoundly influenced the transcriptome of organoid ECs during the vascularization process. While organoid ECs cultured *in vitro* exhibited responses to DNA damage, stress, and growth arrest, those from transplanted organoids displayed enhanced proliferation and differentiation into a fetal artery/afferent arteriole-like phenotype. The transplantation-induced activation of novel transcription factors, such as SOX7, along with exposure to blood flow, likely play pivotal roles in driving these processes. Our findings therefore provide valuable insights into the potential and limitations of endogenous organoid ECs, and identify possible targets to enhance their vascularization potential *in vitro*.

## Methods

### *iPSC maintenance and differentiation*

hiPSC lines reporter MAFB:mTagBFP2 (hiPSC-MAFB)<sup>43</sup> and LUMC0072iCTRL01 were used for kidney organoid generation. LUMC0072iCTRL01 was obtained from the Leiden hiPSC hotel (approving ethics committee: Leiden University Medical Center Ethics Committee, umbrella protocol 13080, detailed information can be found at <https://hpscereg.eu/>). iPSC-MAFB was generated from commercially available fibroblasts (ATCC, sourced from third party suppliers that obtained informed consent). Both cell lines were maintained in Essential 8 medium (E8, Thermo Fisher Scientific) with 0.5% Penicillin-Streptomycin (Thermo Fisher Scientific) on recombinant human Vitronectin (Thermo Fisher Scientific). hiPSC-MAFB was used for the scRNAseq experiments and IF stainings. LUMC0072 for IF stainings only. Cell lines were mycoplasma free. hiPSCs were passaged twice a week using 0.5 mM UltraPure EDTA (Thermo Fisher Scientific). One day before the start of differentiation, they were dissociated to single cells using TrypLE Select (Thermo

Fisher Scientific) and plated at 15,000 – 25,000 cells / cm<sup>2</sup> with the addition of RevitaCell Supplement (ThermoFisher Scientific). During the entire differentiation, hiPSCs were cultured in STEMdiff APEL2 medium (Stem Cell Technologies) with 1% Protein Free Hybridoma Medium II (PFHMII, Thermo Fisher Scientific) and 1% Antibiotic-Antimycotic solution (Thermo Fisher Scientific). From day 0-4, this was supplemented with 8  $\mu$ M CHIR99021 (R&D Systems), and from day 4-7, with 200 ng mL<sup>-1</sup> rhFGF9 (R&D Systems) and 1  $\mu$ g mL<sup>-1</sup> heparin (Sigma Aldrich). On day 7, differentiating cells were treated with an 1 hour 5  $\mu$ M CHIR pulse, dissociated to single cells with Trypsin-EDTA (0.25%, Thermo Fisher Scientific), centrifuged and plated on Transwell 0.4  $\mu$ M pore polyester membranes as pellets of 500,000 cells. Until day 7+5, the developing organoids were cultured in APEL2-medium supplemented with 200 ng mL<sup>-1</sup> rhFGF9 and 1  $\mu$ g mL<sup>-1</sup> heparin (only bottom compartment), and from day 7+5 onwards in APEL2 without supplements. Medium change was performed every 2 days until transplantation on day 7+12 or the end of the experiment on day 7+20.

### ***Transplantation in chicken embryos***

In accordance with Dutch law, approval by the animal welfare committee was not required for these experiments. Detailed methods were previously described <sup>6</sup>. Briefly, Fertilized White Leghorn eggs (*Gallus gallus domesticus*, Drost Loosdrecht B.V.) were incubated at 37 °C. On day 3 of incubation, 3mL of albumen was removed to lower the embryo inside the eggs and a window was cut into the egg shell. One day later (Hamburger Hamilton stage 23), half a kidney organoid on day 7+12 of differentiation was transplanted inside the coelomic cavity of each chicken embryo<sup>44</sup>. On day 5 and 12 of incubation (respectively 1 and 8 days after transplantation), the chicken embryos were euthanized by decapitation and the organoids harvested. Some of the embryos were carefully injected with 20  $\mu$ L of 2,5 mg mL<sup>-1</sup> rhodamine labelled *lens culinaris agglutinin* (LCA) (RL-1042, Vector Laboratories) <sup>45</sup> in the vitelline vein using a glass microcapillary needle before being sacrificed to enable analysis of the vasculature.

### ***Human endothelial cell isolation***

Untransplanted and transplanted organoids generated using the hiPSC-MAFB line were dissociated to single cells at d7+13 and d7+20 of differentiation. At d7+13, 94 untransplanted and 75 bisected transplanted organoids (150 chicken embryos) were dissociated, and at d7+20, 49 untransplanted and 24 bisected transplanted organoids (48 chicken embryos) were used. Organoids were incubated in a collagenase I buffer consisting of 600U ml<sup>-1</sup> collagenase Type I (Worthington) and 0,75U ml<sup>-1</sup> DNase (Sigma

Aldrich) in HBSS with calcium and magnesium (Thermo Fisher Scientific) for 40 min in a water bath at 37°C with repeated pipetting. Cell suspensions were centrifuged for 7 min at 300G and resuspended in a TrypLE buffer consisting of 5U ml<sup>-1</sup> DNase I (Sigma Aldrich) and 4µg ml<sup>-1</sup> heparin (Sigma Aldrich) in 80% TrypLE select 10x (Thermo Fisher Scientific) in DPBS (Thermo Fisher Scientific). They were incubated for another 5 min at 37°C before dissociation was stopped through addition of cold HBSS+/+ with 10% FCS and further diluted with HBSS+/+. Cells were centrifuged for 5 min at 400G and resuspended in wash buffer (PBS + 0,1% BSA).

Viable ECs were identified and sorted on a FACS Aria II or III cell sorter using a staining for human CD31 combined with a viability dye: Organoid cells were incubated with CD31-PE (1:100, BD Biosciences 555446) and viability dye eFluor 780 (1:5000, ThermoFisher Scientific 65-0865-14) in FACS buffer (PBS + 0,1% BSA + 2mM EDTA) for 30 min at 4°C. Viable endothelial cells (d7+13 untransplanted: 23060, transplanted: 6843. D7+20 untransplanted: 6697, transplanted: 36444) were sorted using a FACS Aria II 3L or FACS Aria III 4L (BD Biosciences) and collected in wash buffer. Cells were centrifuged for 6 min at 400G and resuspended in 10X buffer (PBS + 0,04% BSA). Cell number and viability were assessed using a Bio-Rad TC20 cell counter after staining with Trypan Blue. Due to the low number of sorted cells from transplanted d7+13 and untransplanted d7+20 organoids, these were not counted. The single cell suspensions were converted to barcoded scRNA-seq libraries with a targeted cell recovery of 6000 cells / condition using the Chromium Single Cell 3' v3 Library, Gel Bead & Multiplex Kit and Chip Kit (10x Genomics).

### ***Immunofluorescence analysis***

Untransplanted organoids from hiPSC-MAFB and LUMC0072 were fixed in 2% paraformaldehyde (PFA) for 20 min at 4°C, and transplanted organoids in 4% PFA overnight at 4°C. Both were thoroughly washed after fixation and used for whole mount staining. Organoids were permeabilized and blocked in blocking solution (PBS + 0.3% TritonX + 10% donkey serum) for 2 hours. Primary antibodies were diluted in blocking solution and incubated for 24–72 hours. After washing, secondary antibodies in blocking solution were incubated for 2–4 h at room temperature. Kidney organoids were characterized for CD31 and Ki67. Primary antibodies were detected with donkey-α-goat Alexa Fluor 568 and 647, and donkey-α-mouse Alexa Fluor 488. Antibodies and isotype controls were validated in human kidney samples. Nuclei were stained with Hoechst33258 (Thermo Fisher Scientific) and tissues embedded in ProLong Gold Antifade Mountant (Thermo Fisher Scientific) in 35 mm glass bottom dishes (MatTek corporation) or adhesive microscope

slides (StarFrost, Knittel glass). Leica White Light Laser Confocal Microscope TCS SP8 using LAS-X Image software was used for analysis of the tissues.

### ***Kidney organoid culture in hypoxia***

Kidney organoids were generated from hiPSCs in the same manner as described above until day 7+5 or day 7+12 of differentiation. From that moment until the end of the experiment on day 7+20, they were cultured in a hypoxia incubator at 5% O<sub>2</sub>.

### ***Quantification of CD31 positive endothelial cells***

CD31 positive endothelial cells were quantified in whole mount organoids at d7+20. Imaris software was used to calculate the volume of CD31 positive cells, as a percentage of whole organoid volume. A surface of the whole mount organoids was calculated and was used to calculate the volume of the organoid with statistics function in Imaris. Next, a surface was created for the CD31 channel and the volume of this surface was obtained in the same manner. Threshold and minimum number of voxels for CD31 surface generation were set separately for each sample, to be able to correct for differences in background and if necessary, background falsely identified as endothelial cells by the software was removed manually. Graphpad Prism 9.0.1 was used for statistical analysis. Means were compared between groups using a One-way ANOVA. Normality of the distribution was tested and confirmed using the Shapiro-Wilk and Kolmogorov-Smirnov test. Individual data points and mean (SD) are presented.

### ***Deep sequencing and data pre-processing***

The snRNA-seq libraries were sequenced and the reads processed as previously described.<sup>6</sup> Reads were demultiplexed and aligned to the human reference genome only (GRCh38) for both, samples from untransplanted and transplanted organoids, using Cell Ranger (10x Genomics, v3.1.0). Key sequencing metrics are summarized in supplementary data 1.

Raw unfiltered data matrices from the Cell Ranger output were then further processed with R (v4.1.1) and Seurat package (v4.2.0). The following quality control steps were performed for each dataset: (i) genes expressed by less than 10 cells were removed; (ii) cells that expressed fewer than 500 genes were discarded as low-quality cells (supplementary data 1, supplementary Fig. 1a); (iii) cells with a detected number of genes exceeding a “doublet” threshold as listed in supplementary data 1 were excluded (determined by inspecting the cell frequency per total number of genes expressed, for each sample).

Samples were merged resulting in 15,961 cells (supplementary data 1). Dead/dying cells with a fraction of mitochondrial genes >15% were further removed. To identify and remove remaining low-quality cells, data were normalized using the *NormalizeData()* function from Seurat Package, and the top 2000 highly variable genes were identified using *FindvariableFeatures()*. Data were scaled with the *Scaledata()* function and reduced with principal component (PC) analysis using *RunPCA()* function. The top 30 PCs were used for visualization using uniform manifold approximation and projection (UMAP) with the *RunUMAP()* function as implemented in Seurat (min.dist=0.1, n.neighbors=15). Next, a shared nearest-neighbor graph (SNN) was determined using *FindNeighbors()* function on the 30 PCs with “k.param” set at 20, and used to calculate clusters with the *FindClusters()* function with resolution 1 and other settings set as default. Remaining low-quality cell clusters were identified according to the number of genes per cell and number of UMI per cell, and removed, resulting in 12,744 high-quality cells.

## **ScRNAseq data analysis**

### **In silico selection of ECs**

The top 2000 highly variable genes were identified, scaled, and reduced with PC analysis. The top 30 PCs were used for visualization using UMAP with default settings. Clustering was performed as described above with “k.param” set at 30. Top marker genes were calculated with the *Findallmarkers()* function using default settings. Non-EC clusters (negative for *CDH5*, *PECAM1*, *KDR*, *CD34*, *ESM1* genes) including epithelial cells (*KRT19*, *CDH6*, *CLDN3*, *CLDN4*, *APOE*), podocytes (*NPHS1*, *NPSH2*, *MAFB*, *WT1*, *CLIC5*), mesenchymal cells (*COL1A1*, *COL3A1*, *COL6A3*, *POSTN*, *PDGFRB*) and myeloid cells (*PTPRC*, *LYZ*, *MPO*, *MNDA*, *DEFA4*), were removed from the dataset for downstream analysis.

### **EC dataset integration and clustering**

Data were integrated according to the transplantation and timepoint conditions. For each condition, the top 2,500 variable features were identified, and used for integration running the *FindIntegrationAnchors()* function with 50 PC and anchor.features set at 2,500, and the *IntegrateData()* function from the Seurat package. The integrated data were scaled regressing out the percentage of mitochondrial and ribosomal genes, and reduced in 46 PCs that were further used as input for UMAP calculation with “min.dist”=0.1 and “n.neighbors”=50. Clustering was performed as described above with “k.param” set at 12 and the 46 PCs. Top marker genes for each cluster were calculated with the *Findallmarkers()* function, including genes for which  $\text{Log}_2\text{FC} > 0$  only, and using other parameters as default.

## Integration of kidney organoids ECs with human fetal kidney ECs

Publicly available fetal kidney datasets were obtained from GEO and the human cell atlas repositories. All fetal kidney samples were collected with informed consent and ethical approval (supplementary data 14). Only samples containing at least ~100 ECs were retained: GSE102596 (1 sample wk16), GSE112570 (2 samples wk17), GSE114530 (1 sample wk16), GSE124472 (1 sample wk15, 2 samples wk17), GSE139280 (2 samples wk14) and ERP120466 (2 samples wk8, 1 sample wk9, 1 sample wk12, 1 sample wk14, 1 sample wk16). All count data were processed using the *NormalizeData()*, *FindVariableFeatures()*, *ScaleData()*, *RunPCA()*, *RunUMAP()* functions using number of PCs determined according to the output from the *ElbowPlot()* function from the Seurat package, with default settings. EC cluster(s) were obtained from *FindNeighbors()* function with “k.param” set at 30 and *FindClusters()* function using default settings, and by assessing the expression of canonical EC marker genes except for the week 16 sample from GSE114530, for which the “End” annotation was used. EC clusters from each dataset were subset and merged using *subset()* and *merge()* functions, respectively. Samples were further integrated using the canonical correlation analysis from the Seurat pipeline with 20 dimensions, 2,000 variable features, “k.filter” set at 150, and “k.weight” set at 90, from the *FindIntegrationAnchors()* and *IntegrateData()* functions. Integrated data were scaled, and dimensionally reduced to 30 dimensions. The first 8 dimensions were used to generate UMAP plot and identify nearest neighbors with “k.param” set at 30. Clusters were identified with resolution set at 1 from the *FindClusters()* function, with other default parameters. After removal of a cluster representing doublets, the integration pipeline was iterated with EC singlets only, per sample. Parameters used were 15 dimensions, 2,000 anchor features, and k.filter and k.weight set at 140 and 90, respectively. Integrated data were again scaled and dimensionally reduced to 30 dimensions. For preparing the final UMAP, the first 7 dimensions were used with “min.dist” parameter set at 0.1 in the *RunUMAP()* function. Clustering was performed again as previously described with resolution set to 0.8. Marker genes for each cluster were calculated with the *FindAllMarkers()* function setting “only.pos” to TRUE and the other settings used as default. Cluster annotation was based on canonical marker gene expression. This fetal kidney EC dataset was further integrated with the EC dataset from transplanted kidney organoids collected at d7+20. Briefly, gene annotation from the fetal kidney EC dataset was first updated from the GRCh37 to the GRCh38 reference genome using the biomaRt package (v2.58.2). The datasets were then integrated using the canonical correlation analysis from the Seurat pipeline with 20 dimensions, 2,000 anchor features and both “k.filter” and “k.weight” parameters set at 90 for the *FindIntegrationAnchors()* and *IntegrateData()* functions. Integrated data were scaled regressing out the percentage of mitochondrial and ribosomal genes and reduced to 50 PC dimensions. The 20 dimensions were used to generate the UMAP with “min.dist” set at 0.2 and “n.neighbors” at 30.

## Comparison of kidney organoid EC clusters with fetal kidney EC clusters

Per cluster average expression of the integrated scaled data from both the kidney organoid ECs collected at d7+20 and fetal kidney ECs was used to assess similarity. A correlation matrix was generated using the *cor()* function. Output was visualized as heatmap (see Visualization paragraph below).

Marker genes were identified for the “Artery 2” cluster from kidney organoid ECs collected at d7+20 and “kidney artery-afferent arteriole” cluster from fetal kidney ECs using the *FindMarkers()* function for each dataset, with running a MAST test setting the number UMIs per cell as latent variable, and “only.pos” parameter to TRUE. Only significant marker genes were retained (adjusted p-value < 0.05). Shared marker genes were identified using the *intersect()* function.

## Geneset enrichment analysis (GSEA)

Differentially expressed genes in each transplantation and timepoint combination were obtained using the *FindAllMarkers()* function using the MAST test, setting the number of UMIs per cell as latent variable, and the “logfc.threshold” and “min.pct” parameters to 0. GSEA was performed on the ranked genes using *gseGO()* function from ClusterProfiler package (v.4.10.0). pValueCutoff was set to 0.05 and the biological process gene ontology was used. GO Terms were simplified using the *GOSemSim* package (v2.28.1) and the *simplify()* function with measure and cutoff parameters set to “Rel” and 0.05, respectively. The top 10 upregulated genesets were filtered and visualized using the *dotplot()* function from the ClusterProfiler package.

## Geneset expression analysis: module score calculation

Module scores were calculated for each cell to identify proliferating ECs in G1S/S or G2M/M cell cycle stages, and artery, vein and lymphatic EC clusters. Module scores for proliferative ECs were calculated using *CellCycleScoring()* function from the Seurat package using canonical G1S/S and G2M/M cell cycle genes, as listed in Seurat. Calculation of the other module scores was performed using the *AddModuleScore()* function and based on the expression of the canonical marker genes *NRP1*, *SEMA3G*, *MECOM*, *GJA4*, *GJA5*, *HEY2*, *JAG1*, *JAG2*, *HES4*, *EFNB2*, *SOX17*, *EPAS1* and *BMX* for artery ECs; *APLNR*, *NR2F2*, *NRP2*, *PLVAP* and *EPHB4* for vein ECs; and *FLT4*, *THY1*, *TBX1* and *PROX1* for lymphatic ECs. Quiescent or migrating EC clusters displaying low artery, vein and lymphatic module scores were labelled as capillary ECs.

For the assessment of the transcriptional response to laminar shear stress, geneset was downloaded from the molecular signature database MSigDB (<https://www.gsea-msigdb.org/gsea/index.jsp>) and the *AddModuleScore()* function was used.

The GOBP\_RESPONSE\_TO\_LAMINAR\_FLUID\_SHEAR\_STRESS geneset included the following genes *KLF2*, *ACE*, *ABCA1*, *MIR126*, *SMAD6*, *SMAD7*, *ASS1*, *NFE2L2*, *MAPK7*, *MAP2K5*, *SREBF2*, *TGFB3* and *KLF4*.

### Geneset variation analysis (GSVA)

The EC dataset from the Tabula Sapiens study <sup>14</sup>was downloaded from the UCSC cell browser (<https://cells.ucsc.edu/?ds=tabula-sapiens+func-compart>), and used to generate a Seurat object with the *CreateSeuratObject()* function. Count data were normalized using *NormalizeData()* function. To identify tissue-specific EC marker genes, the *FindAllMarkers()* function setting the “only.pos” to TRUE, was used with selecting “organ\_tissue” as grouping variable. Only significantly upregulated marker genes (adjusted p-value<0.05, log2FC>0.5) were retained for each tissue. Moreover, marker genes identified in more than one tissue were discarded. Tissue ECs defined by less than 30 marker genes were removed from the analysis. Finally, only genes also present in the kidney organoid EC dataset were retained, resulting in marker genes and tissues listed in Supplementary Data 10. GSVA was performed with these gene lists and the normalized data matrix of the kidney organoid ECs using the *gsva()* function from the GSVA package (v1.50.5).

### Correlation analysis & hierarchical clustering

For correlation analysis of kidney organoid EC conditions, briefly, count data matrix was exported from the Seurat object using the *GetAssayData()* function (selected assay “RNA”) and uploaded in the BIOMEX software (v1.5 - <https://carmelietlab.sites.vib.be/en/biomex>)<sup>46</sup> altogether with the corresponding metadata information. Data were normalized (“Standard” parameter) and (auto)scaled within BIOMEX. They were further grouped according to the transplantation and timepoint combinations, and highly variable genes were used to determine correlation coefficients between conditions. Hierarchical clustering was calculated using Euclidian distance and complete agglomeration method.

### Visualization

Gene expression dot plots and heatmaps were created with R using the *DotPlot()* and *Heatmap()* functions from the Seurat and ComplexHeatmap packages (v2.18.0),

respectively, except for the correlation heatmap, which was prepared within BIOMEX. For gene expression heatmaps prepared with the ComplexHeatmap package, briefly, the averaged expression profiles per each cluster and for all genes were calculated using the *AverageExpression()* function from Seurat package. Next, scaled data were obtained from the RNA assay using *GetAssayFunction()* function and selected gene data were extracted from the resulting matrix. These values were used as input for the *Heatmap()* function from the ComplexHeatmap package. UMAP plots were generated using *DimPlot()* and *FeaturePlot()* functions from the Seurat package, for metadata and gene expression visualization, respectively. Violin plots were generated using *VlnPlot()* from the Seurat package. Proportions of the different EC populations were visualized as pie charts or bar plots with the ggplot2 package (v3.4.4).

### **Analysis of kidney organoid chicken ECs**

Processed chicken scRNA-seq data from transplanted organoids at day 7+20 were downloaded from ArrayExpress repository (accession number E-MTAB-11429) and endothelial cells were subset according to the metadata information. After removal of red blood cell-EC doublets, the standard pipeline described above was used. Briefly, data were log-normalized, and the top 2,000 highly variable genes were scaled and used as input for dimensionality reduction via PCA and UMAP (first 12 principal components used, and “min.dist” parameter set at 0.1). Unsupervised clustering was performed as described above with resolution set at 0.6. Cluster-specific marker genes were identified with the *FindAllMarkers()* function from the Seurat package, with “only.pos” parameter set to TRUE. Chicken EC clusters were annotated according to canonical markers and identified top marker gene expression.

### ***Bulk RNA-seq data analysis of iPSC-ECs exposed to laminar flow vs static culture***

Raw data from NCRM1 iPSC-ECs were obtained from the BioStudies repository (E-MTAB-8392) and pre-processed as described previously<sup>17</sup>. The NCRM1 cell line is commercially available through RUCDR Infinite Biologics (Piscataway, New Jersey), and was generated by reprogramming of CD34+ cord blood cells using episomal vectors with approval of the institutional review board of the involved hospital. Counts per million were calculated using *cpm()* function from the EdgeR package (v4.0.14). Ensembl IDs were converted to gene symbols using the biomaRt package. *JAG1* expression dot plot was generated in GraphPad Prism (10.2.3). Statistical difference was assessed using paired Student's t-test (significant if p-value<0.05) as implemented in GraphPad Prism.

## Data availability

Both raw and processed sequencing data are available upon request to the European Genome-Phenome Archive (EGA): Study EGAS50000001068, Dataset EGAD50000001555.

## Code availability

Custom code is available upon reasonable request.

## Acknowledgements

We are grateful to Melissa Little (Murdoch Children's Research Institute, Melbourne, Australia) for providing the cell line iPSC-MAFB, and Christian Freund (hiPSC core facility, LUMC, Leiden, the Netherlands) for providing hiPSC line LUMC0072. We acknowledge the support of Saskia van der Wal-Maas (Department of Anatomy & Embryology, LUMC, Leiden, the Netherlands), Conny van Munsteren (Department of Anatomy & Embryology, LUMC, Leiden, the Netherlands), Manon Zuurmond (LUMC, Leiden, the Netherlands), George Galaris (LUMC, Leiden, the Netherlands), Lonneke Gaykema (LUMC, Leiden, the Netherlands), Loes Wiersma (LUMC, Leiden, the Netherlands), and Lin Xie (MGI, BGI-Shenzhen).

## References

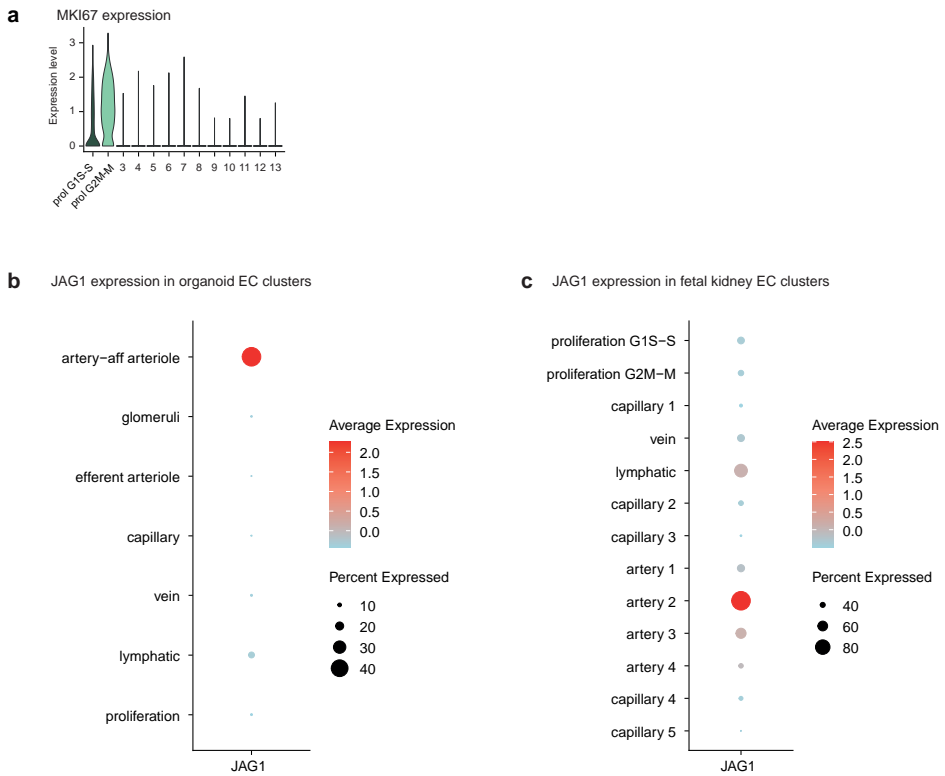
- 1 Dumas, S. J. Single-Cell RNA Sequencing Reveals Renal Endothelium Heterogeneity and Metabolic Adaptation to Water Deprivation. *JASN* (2019).
- 2 Molema, G. & Aird, W. C. Vascular heterogeneity in the kidney. *Semin Nephrol* **32**, 145-155 (2012). <https://doi.org/10.1016/j.semnephrol.2012.02.001>
- 3 Jourde-Chiche, N. et al. Endothelium structure and function in kidney health and disease. *Nat Rev Nephrol* (2019). <https://doi.org/10.1038/s41581-018-0098-z>
- 4 Brunskill, E. W. et al. Genes that confer the identity of the renin cell. *J Am Soc Nephrol* **22**, 2213-2225 (2011). <https://doi.org/10.1681/ASN.2011040401>
- 5 van den Berg, C. W. et al. Renal Subcapsular Transplantation of PSC-Derived Kidney Organoids Induces Neo-vasculogenesis and Significant Glomerular and Tubular Maturation In Vivo. *Stem Cell Reports* **10**, 751-765 (2018). <https://doi.org/10.1016/j.stemcr.2018.01.041>
- 6 Koning, M. et al. Vasculogenesis in kidney organoids upon transplantation. *NPJ Regen Med* **7**, 40 (2022). <https://doi.org/10.1038/s41536-022-00237-4>
- 7 Aibar, S. et al. SCENIC: single-cell regulatory network inference and clustering. *Nature Methods* **14**, 1083+ (2017). <https://doi.org/10.1038/Nmeth.4463>
- 8 Downes, M. & Koopman, P. SOX18 and the transcriptional regulation of blood vessel development. *Trends Cardiovasc Med* **11**, 318-324 (2001). [https://doi.org/10.1016/s1050-1738\(01\)00131-1](https://doi.org/10.1016/s1050-1738(01)00131-1)
- 9 Wei, G. et al. Ets1 and Ets2 are required for endothelial cell survival during embryonic angiogenesis. *Blood* **114**, 1123-1130 (2009). <https://doi.org/10.1182/blood-2009-03-211391>
- 10 Zhu, Q., Kim, Y. H., Wang, D., Oh, S. P. & Luo, K. SnoN facilitates ALK1-Smad1/5 signaling during embryonic angiogenesis. *J Cell Biol* **202**, 937-950 (2013). <https://doi.org/10.1083/jcb.201208113>
- 11 Hermkens, D. M. et al. Sox7 controls arterial specification in conjunction with hey2 and efnb2 function. *Development* **142**, 1695-1704 (2015). <https://doi.org/10.1242/dev.117275>
- 12 Lilly, A. J., Mazan, A., Scott, D. A., Lacaud, G. & Kouskoff, V. SOX7 expression is critically required in FLK1-expressing cells for vasculogenesis and angiogenesis during mouse embryonic development. *Mech Dev* **146**, 31-41 (2017). <https://doi.org/10.1016/j.mod.2017.05.004>
- 13 Ryan, A. R. et al. Vascular deficiencies in renal organoids and ex vivo kidney organogenesis. *Dev Biol* **477**, 98-116 (2021). <https://doi.org/10.1016/j.ydbio.2021.04.009>
- 14 Tabula Sapiens, C. et al. The Tabula Sapiens: A multiple-organ, single-cell transcriptomic atlas of humans. *Science* **376**, eabl4896 (2022). <https://doi.org/10.1126/science.abl4896>
- 15 Fang, J. S. et al. Shear-induced Notch-Cx37-p27 axis arrests endothelial cell cycle to enable arterial specification. *Nat Commun* **8**, 2149 (2017). <https://doi.org/10.1038/s41467-017-01742-7>
- 16 Rodriguez, F. S. et al. Jagged1 is a Notch-independent mechanotransducer in endothelial cells. *bioRxiv*, 2024.2011.2014.623558 (2024). <https://doi.org/10.1101/2024.11.14.623558>
- 17 Tiemeier, G. L. et al. Closing the Mitochondrial Permeability Transition Pore in hiPSC-Derived Endothelial Cells Induces Glycocalyx Formation and Functional Maturation. *Stem Cell Reports* **13**, 803-816 (2019). <https://doi.org/10.1016/j.stemcr.2019.10.005>
- 18 Jankovic, B. D. et al. Immunological capacity of the chicken embryo. I. Relationship between the maturation of lymphoid tissues and the occurrence of cell-mediated immunity in the developing chicken embryo. *Immunology* **29**, 497-508 (1975).

- 19 Alkie, T. N. et al. Development of innate immunity in chicken embryos and newly hatched chicks: a disease control perspective. *Avian Pathol* **48**, 288-310 (2019). <https://doi.org/10.1080/03079457.2019.1607966>
- 20 Hamburger, V. Morphogenetic and axial self-differentiation of transplanted limb primordia of 2-day chick embryos. *Journal of Experimental Zoology* **77**, 379-399 (1938).
- 21 Rawles, M. E. Transplantation of normal embryonic tissues. *Ann N Y Acad Sci* **55**, 302-312 (1952).
- 22 Rawles, M. E. The Development of Melanophores from Embryonic Mouse Tissues Grown in the Coelom of Chick Embryos. *Proc Natl Acad Sci U S A* **26**, 673-680 (1940).
- 23 Sharmin, S. et al. Human Induced Pluripotent Stem Cell-Derived Podocytes Mature into Vascularized Glomeruli upon Experimental Transplantation. *J Am Soc Nephrol* **27**, 1778-1791 (2016). <https://doi.org/10.1681/ASN.2015010096>
- 24 Bantounas, I. et al. Generation of Functioning Nephrons by Implanting Human Pluripotent Stem Cell-Derived Kidney Progenitors. *Stem Cell Reports* **10**, 766-779 (2018). <https://doi.org/10.1016/j.stemcr.2018.01.008>
- 25 Tran, T. et al. In Vivo Developmental Trajectories of Human Podocyte Inform In Vitro Differentiation of Pluripotent Stem Cell-Derived Podocytes. *Developmental Cell* **50**, 102-+ (2019). <https://doi.org/10.1016/j.devcel.2019.06.001>
- 26 ACUC. ACUC Guideline: The Use and Euthanasia Procedures of Chicken/Avian Embryos., <<https://www.cpp.edu/research/research-compliance/iacuc/docs/iacuc-guidelines-on-euthanasia-of-chicken-and-embryos.pdf>> (2012).
- 27 De Bock, K. et al. Role of PFKFB3-driven glycolysis in vessel sprouting. *Cell* **154**, 651-663 (2013). <https://doi.org/10.1016/j.cell.2013.06.037>
- 28 Xu, Y. et al. Endothelial PFKFB3 plays a critical role in angiogenesis. *Arterioscler Thromb Vasc Biol* **34**, 1231-1239 (2014). <https://doi.org/10.1161/ATVBAHA.113.303041>
- 29 Rohlenova, K., Veys, K., Miranda-Santos, I., De Bock, K. & Carmeliet, P. Endothelial Cell Metabolism in Health and Disease. *Trends Cell Biol* **28**, 224-236 (2018). <https://doi.org/10.1016/j.tcb.2017.10.010>
- 30 De Bock, K., Georgiadou, M. & Carmeliet, P. Role of endothelial cell metabolism in vessel sprouting. *Cell Metab* **18**, 634-647 (2013). <https://doi.org/10.1016/j.cmet.2013.08.001>
- 31 Schumacher, A. et al. Enhanced Microvasculature Formation and Patterning in iPSC-Derived Kidney Organoids Cultured in Physiological Hypoxia. *Front Bioeng Biotechnol* **10**, 860138 (2022). <https://doi.org/10.3389/fbioe.2022.860138>
- 32 Walls, J. R., Coultas, L., Rossant, J. & Henkelman, R. M. Three-dimensional analysis of vascular development in the mouse embryo. *PLoS One* **3**, e2853 (2008). <https://doi.org/10.1371/journal.pone.0002853>
- 33 Hou, S. et al. Heterogeneity in endothelial cells and widespread venous arterIALIZATION during early vascular development in mammals. *Cell Res* **32**, 333-348 (2022). <https://doi.org/10.1038/s41422-022-00615-z>
- 34 Maggiore, J. C. et al. A genetically inducible endothelial niche enables vascularization of human kidney organoids with multilineage maturation and emergence of renin expressing cells. *Kidney Int* (2024). <https://doi.org/10.1016/j.kint.2024.05.026>
- 35 Follert, P., Grosse-Segerath, L. & Lammert, E. Blood flow-induced angiocrine signals promote organ growth and regeneration. *Bioessays*, e2400207 (2024). <https://doi.org/10.1002/bies.202400207>

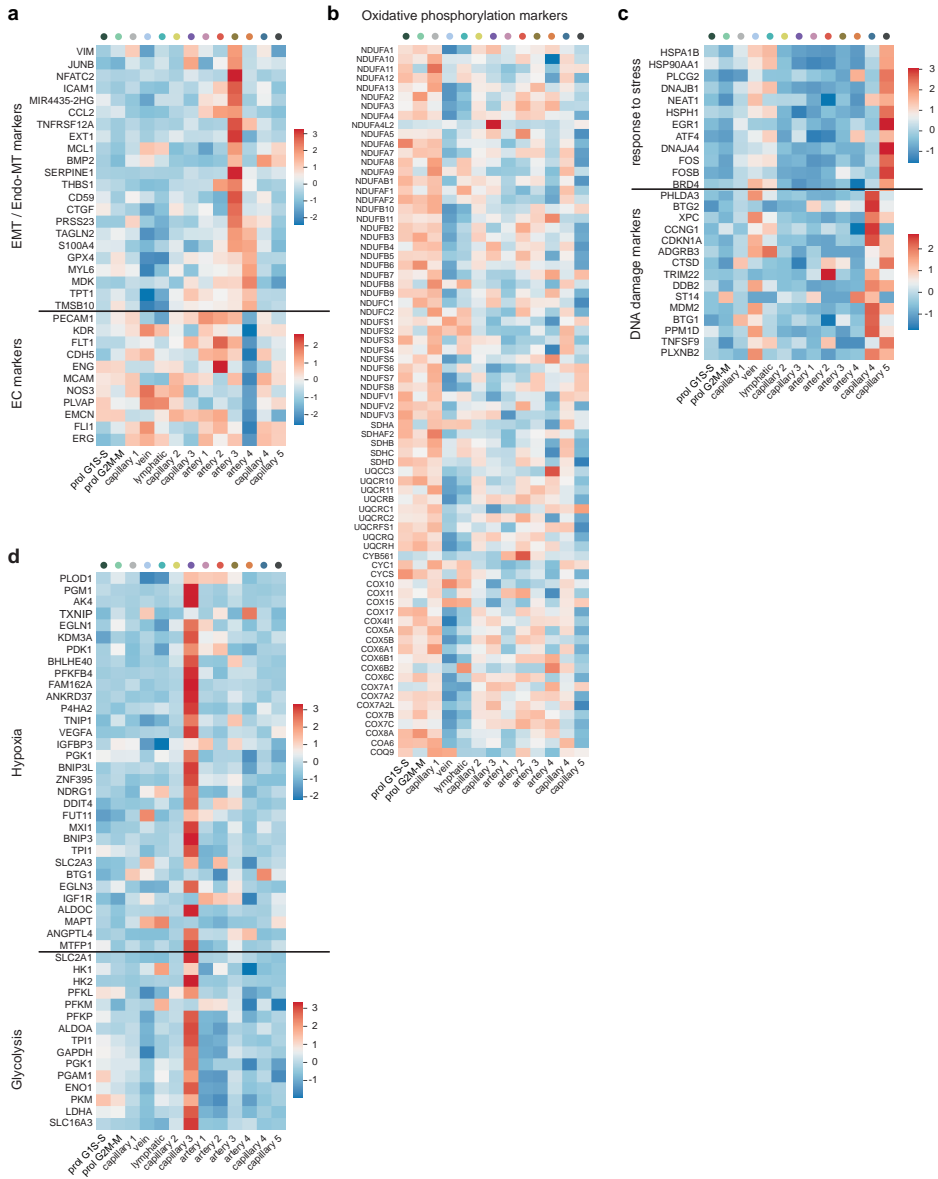
- 36 Bishop, D., Schwarz, Q. & Wiszniak, S. Endothelial-derived angiocrine factors as instructors of embryonic development. *Frontiers in Cell and Developmental Biology* **11** (2023). [https://doi.org/ARTN 1172114 10.3389/fcell.2023.1172114](https://doi.org/ARTN%201172114%2010.3389/fcell.2023.1172114)
- 37 Lorenz, L. et al. Mechanosensing by beta1 integrin induces angiocrine signals for liver growth and survival. *Nature* **562**, 128-132 (2018). <https://doi.org/10.1038/s41586-018-0522-3>
- 38 Homan, K. A. et al. Flow-enhanced vascularization and maturation of kidney organoids in vitro. *Nat Methods* **16**, 255-262 (2019). <https://doi.org/10.1038/s41592-019-0325-y>
- 39 Menéndez, A. B. C. et al. Creating a kidney organoid-vasculature interaction model using a novel organ-on-chip system. *Sci Rep-Uk* **12** (2022). [https://doi.org:ARTN 20699 10.1038/s41598-022-24945-5](https://doi.org/ARTN%2020699%2010.1038/s41598-022-24945-5)
- 40 Zhang, H., Yamaguchi, T., Kokubu, Y. & Kawabata, K. Transient ETV2 Expression Promotes the Generation of Mature Endothelial Cells from Human Pluripotent Stem Cells. *Biol Pharm Bull* **45**, 483-490 (2022). <https://doi.org/10.1248/bpb.b21-00929>
- 41 De Val, S. & Black, B. L. Transcriptional Control of Endothelial Cell Development. *Developmental Cell* **16**, 180-195 (2009). <https://doi.org/10.1016/j.devcel.2009.01.014>
- 42 Behrens, A. N. et al. Is Regulated by ETV2 During Cardiovascular Development. *Stem Cells and Development* **23**, 2004-2013 (2014). <https://doi.org/10.1089/scd.2013.0525>
- 43 Vanslambrouck, J. M. et al. A Toolbox to Characterize Human Induced Pluripotent Stem Cell-Derived Kidney Cell Types and Organoids. *J Am Soc Nephrol* (2019). <https://doi.org/10.1681/ASN.2019030303>
- 44 Hamburger, V. & Hamilton, H. L. A series of normal stages in the development of the chick embryo. 1951. *Dev Dyn* **195**, 231-272 (1992). <https://doi.org/10.1002/aja.1001950404>
- 45 Jilani, S. M. et al. Selective binding of lectins to embryonic chicken vasculature. *J Histochem Cytochem* **51**, 597-604 (2003).
- 46 Taverna, F. et al. BIOMEX: an interactive workflow for (single cell) omics data interpretation and visualization. *Nucleic Acids Res* **48**, W385-W394 (2020). <https://doi.org/10.1093/nar/gkaa332>



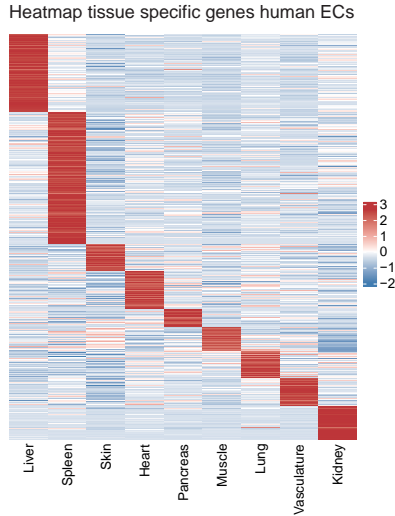
**Supplementary figure 1:** **a** UMAP visualization of (left) all enriched human cells and selection of high-quality cells (blue: high-quality cells, grey: low-quality cells and doublets), and (right) number of detected genes per cell. **b** Left: UMAP visualization of a total of 12,744 high quality cells color-coded by cell type: endothelial cells (large majority), epithelial cells, mesenchymal cells, podocytes, myeloid cells. Right: UMAP plots color-coded by the expression level of CDH5, PECAM1, NPHS2, EPCAM, COL1A2, LYZ. **c** Dot plot representing marker gene expression in the different cell clusters. Dot size indicates proportion of cells in cluster expressing a gene, color intensity indicates the level of expression. **d** UMAP visualization of all high quality human cells (grey) and selection of high quality ECs (blue) .



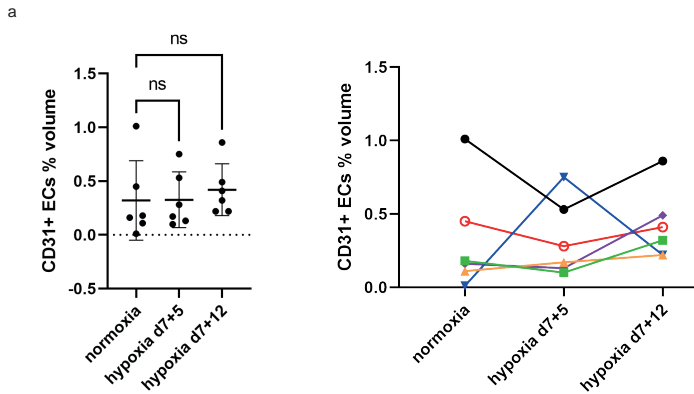
**Supplementary figure 2:** **a** Violin plot visualization of the expression level of MKI67 gene per EC cluster. The G1S-S as well as the G2M-M cluster express MKI67, with higher expression level in the G2M-M cluster. **b** Violin plot visualization of the expression level of JAG1 in organoid EC subclusters. **c** Violin plot visualization of the expression level of JAG1 in fetal kidney EC clusters.



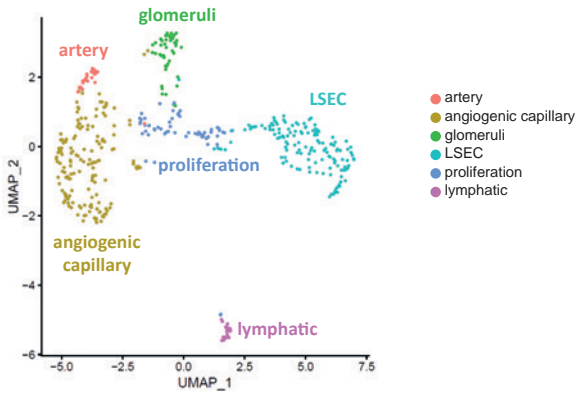
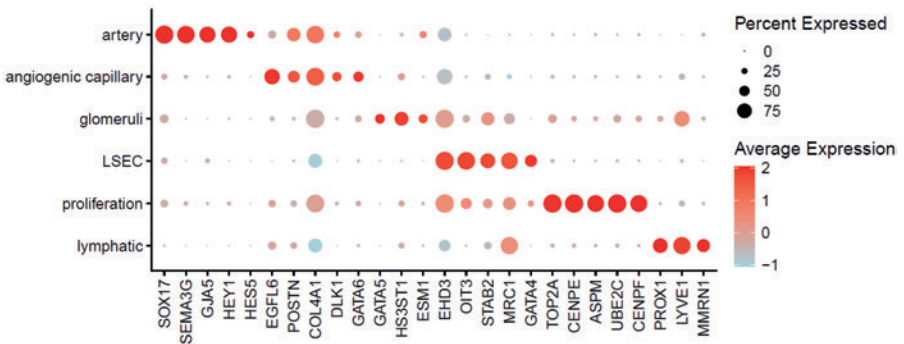
**Supplementary figure 3:** a Heatmap visualization of the expression of EMT / endo-MT marker genes (top) and EC marker genes (bottom) per EC cluster. Scale: z-score of the gene expression level. b Heatmap visualization of the expression of oxidative phosphorylation genes per EC cluster. Scale: z-score of the gene expression level. c Heatmap visualization of the expression of response to stress (top) and DNA damage (bottom) genes per EC cluster. Scale: z-score of the gene expression level. d Heatmap visualization of the expression of hypoxia (top) and glycolysis (bottom) genes per EC cluster. Scale: z-score of the gene expression level.



**Supplementary figure.4:** Heatmap visualization of tissue specific genes of human ECs from different organs. Scale: z-score of the gene expression level



**Supplementary figure 5:** Quantification of CD31 positive ECs as percent volume of organoid volume in whole mount untransplanted organoids at d7+20, after culture in normoxia or in hypoxia (5%) starting from d7+5 or d7+12 of differentiation. n=6 organoids per condition. Left: There is no significant difference in EC volume between organoids cultured in normoxia and those cultured in hypoxia. Data are presented as individual data points, mean (SD). Means were compared between groups using a One-way ANOVA. Right: Alternative visualization demonstrating similar EC percent volume in normoxia and hypoxia in organoids for each differentiation.

**a** Chicken EC clusters transplanted d7+20 organoids**b** Marker gene expression in chicken EC clusters

**Supplementary figure 6: a** UMAP visualization of all chicken ECs from transplanted kidney organoids at day 7+20, color-coded by cluster. 6 subclusters were distinguished: artery, angiogenic capillary, glomeruli, liver sinusoidal endothelial cells (LSEC), proliferation and lymphatic. **b** Dot plot representing marker gene expression in chicken EC clusters. Dot size indicates proportion of cells in a cluster expressing a gene, color intensity indicates the level of expression.

**Supplementary tables and movies can be accessed through the following QR code:**



